[Frontiers In Bioscience, Elite, 10, 143-154, January 1, 2018]

RPS6KA4/*MIR1237* and *AURKC* promoter are differentially methylated in Wilms' tumor

Hanna S Pereira[1], Sheila Coelho Soares Lima[1], Paulo Silvestre de Faria[1], Leila Cabral de Almeida Cardoso[1,2], Héctor Nicolás Seuánez[1,3]

[1]Instituto Nacional de Câncer Jose Alencar Gomes da Silva, Rua André Cavalcanti 37, Rio de Janeiro, Rio de Janeiro, Brazil, [2]Instituto Fernandes Figueira, FIOCRUZ, Avenida Rui Barbosa 716, Rio de Janeiro, Rio de Janeiro, Brazil, [3]Departamento de Genética, Instituto de Biologia, Universidade Federal do Rio de Janeiro, Cidade Universitária, 21941-901 Rio de Janeiro, Rio de Janeiro, Brazil

TABLE OF CONTENTS

1. ABSTRACT

Wilms' tumor (WT) is the most frequent renal cancer in childhood, the occurrence of which is characterized by a relatively low frequency of associated mutations. While epigenetic alterations have been postulated to play a relevant role in the emergence of this tumor, the mechanisms involved in WT development remain largely unknown. In this study, the DNA methylation profile of WT was characterized with Beadchip array. Comparisons between WT with normal kidney identified 827 differentially methylated regions, most of which were attributable in hypermethylation in CpG islands. Among affected genes, *WT1* and *TP73* showed altered enhancers where hypermethylation was validaded by pyrosequencing. Thirty differentially methylated regions (DMRs) were identified in WT as compared to normal kidney, two of which were previously described. Two novel DMRs, located in *RPS6KA4*/*MIR1237* and the *AURKC* promoter, were found to be hypermethylated in WT. Altogether, our data reinforced the relevance of alterations of DNA methylation in WT, highlighting the complex nature of these alterations that affect promoter regions as well as enhancers, UTRs and gene bodies.

2. INTRODUCTION

Wilms' tumor (WT) is the most common renal tumor in childhood with a prevalence of 1 in 10,000 newborns (1). WT is derived from pluripotent renal precursors and the ensuing undifferentiated blastemal cells, primitive epithelial structures and stromal components, resulting in a classically triphasic histology (2,3). These precursor components, known as nephrogenic rests (NR), are present in 40% of unilateral WT and in almost 100% of bilateral WT (4). Treatment is determined by stage and histological classification, with different protocols among countries. The International Society of Pediatric Oncology (SIOP) and the Children's Oncology Group (COG) presently recommend the most widely used protocols in European countries and North America, respectively (1,5).

Few genes and low mutation frequencies have been associated with WT and increased risk for tumor development and progression: *WT1* (Wilms' tumor 1 gene, in 12% of tumors), *CTNNB1* (Cadherin-associated Protein Beta 1, in 15%) (6), *WTX* (APC Membrane Recruitment Protein 1, in 18%) (7), *DROSHA* (Drosha - Ribonuclease Type III, in 12%)

(8), and *TP53* (Tumor Protein 53, in 5%) (9), while in approximately 65% of tumors somatic mutations are not present (10). However, 69% of sporadic WT exhibit epigenetic alterations in the imprinted *IGF2/H19* locus (Insulin-like Growth Factor 2/H19, imprinted maternally expressed transcript, non-protein coding) located in 11p15, while DMRH19 hypermethylation was the most frequent finding, leading to *IGF2* biallelic expression (6).

But despite these associations, the mechanisms leading to the genesis and progression of WT still remain poorly understood. A study of the methylome of 22 tumors and normal adjacent tissues identified three differentially methylated regions (DMRs) with hypermethylation, albeit unrelated to cell subtypes when compared with adjacent renal tissue. Two DMRs located in chromosome 6 were hypermethylated in embryonic blastema and in all tumors, but showed intermediate methylation levels in nephrogenic rests, indicating that epigenetic alterations of these regions played a more relevant role than somatic mutations in WT development. One of these DMRs, with increased methylation levels, was tracked in cell-free circulating DNA for monitoring tumor response to pre-operative chemotherapy, pointing to its potential utilization as a WT biomarker (11).

Another study, based on genome-wide comparative methylation analysis of NR, WTs and normal kidneys (NK), showed different profiles between tissue types and increased variability in both NR and WT samples compared to NK. Additionally, loss of methylation (LOM) was observed in key renal development genes while tumor suppressor genes were inactivated by hypermethylation in tumor samples (10). Constitutional and somatic 11p15 epigenetic alterations have also been reported in WT cohorts (12,13), while several other genes and genomic components were also found to be affected by methylation alterations in WT, like the tumor suppressor gene *RASSF1A* (Ras association domain family 1 isoform A) (14), imprinted genes like *NNAT* (Neuronatin), *WT1* antisense regulatory region (15,16) and pericentromeric satellite regions of chromosome 1 (17).

In view of the relevance of epigenetic changes in carcinogenesis and tumor progression (10, 11, 18), we carried out a study of genome-wide methylation to verify genes and/or DMRs potentially involved in WT development and progression.

3. MATERIAL AND METHODS

3.1. Samples

Twenty seven WT patients were included in this study following approval by the Ethics Committee of Instituto Nacional de Câncer (Brazil), in accordance with the ethical standards of the Helsinki Declaration. All parents or guardians signed an informed consent on behalf of their children. Tumor samples were divided in a training cohort (N = 10) analyzed with BeadChip array and a validation cohort (N = 17) in which findings were confirmed by pyrosequencing.

All tumor samples were collected from primary tumors of patients treated with the same neoadjuvant chemotherapy following the SIOP WT 2001 trial protocol (19). Clinical and pathology data are shown in Table 1. Patients were mostly male (68%) and diagnosed at a median age of 47 months (12-137). Unilateral WT was present in most cases (80%) and tumors were classified in different stages according to SIOP: I (40%), II (25%) and III (35%). Normal kidney samples from five stillborn infants, provided by the Pathology Division of Instituto Fernandes Figueira-FIOCRUZ (IFF/FIOCRUZ, Brazil) were used as controls following approval by the IFF/FIOCRUZ Ethics Committee.

3.2. Genome-wide DNA methylation analysis with Infinium® Human Methylation 450K Beadchip

Tumor samples from 10 patients and two normal kidneys were analyzed. DNA was isolated from fresh tumor samples following standard procedures (20). A total of 500 ng of genomic DNA was treated with sodium bisulfite with EZ DNA Methylation-Gold Kit (Zymo Research D5006) following the manufacturer's instructions for Infinium assays. DNA methylation profiling was carried out with the Infinium HumanMethylation450k BeadChip array (Illumina WG – 314-1003) following the manufacturer's instructions. Beadchips were subsequently scanned with iScan Array Scanning System (Illumina). All internal controls were evaluated with the methylation module of GenomeStudio Software (Illumina). All samples were found to be of appropriate quality. The .idat files were used for subsequent analyses.

3.3. Beadchip data processing and statistical analyses

All analyses were performed with RStudio Software (21). Firstly, the .idat files of each sample were imported (22) following removal of probes containing known SNPs with allele frequencies higher than 5% in the general population and cross-reactive probes (23). Moreover, probes with detection p below 0.0.5 were removed (24). Following color bias adjustment using smooth quantile normalization (25), correction for probe bias was carried out (24).

Methylation levels were expressed as beta-values representing the ratio of intensities between methylated and unmethylated signals, and M-values,

Table 1. Clinical and pathological characteristics of WT patients included in the study

Patient ID	Age at diagnosis (months)	Gender	Laterality	SIOP Tumor Stage
P11	136	M	U	III
P12	90	M	U	III
P14	59	M	U	I
P15	62	F	U	I
P16	29	M	B	I
P17	50	M	B	NA
P18	36	M	U	I
P19	48	F	U	NA
P20	137	M	U	NA
P23	57	M	U	III
P24	13	F	U	I
P25	42	M	U	II
P27	61	M	B	NA
P28	67	M	U	I
P31	34	F	B	I
P34	35	F	U	II
P37	47	M	U	II
P38	19	F	U	III
P40	28	M	U	III
P41	25	M	U	III
P42	56	M	U	II
P43	25	M	U	III
P47	21	M	U	II
P51	48	F	U	I
P54	12	F	B	NA
P55	NA	NA	NA	NA

Abbreviations: F: female; M: Male; B: bilateral; U: unilateral; NA: data not available

or logarithmic transformed beta-values. Beta-values were used for generating multi-dimensional scaling (MDS) plots showing a 2-D projection of distances between samples (26). M-values were used for linear models fit for normal kidney *vs* tumor comparisons; p-values were adjusted for multiple testing according to the Benjamini and Hochberg´s method (27). Differentially methylated probes (DMPs) with adjusted p estimates below 0.0.5 were considered to be statistically significant.

Following identification of the methylation status of each probe, adjacent probes were merged to form continuous regions. Differentially methylated regions (DMRs) were identified by comparing regions with at least five probes and gaps no larger than 2,000 nt between any two adjacent probes. Two adjacent DMRs with gaps with 100 or less nucleotides were merged. DMRs were considered to be statistically significant between normal kidney and WT samples when adjusted p value was lower than 0.0.5) (28).

Chromosome enrichment of DMP was determined by Fisher's exact test (p below 0.0.5).

3.4. Pyrosequencing

Validation of BeadChip findings was carried out by pyrosequencing of CpG sites of five genes found to be hypermethylated in tumor samples. In addition to the 10 samples analyzed with Beadchip, an independent set of 17 tumors was analyzed for corroborating BeadChip findings. Five normal kidney samples were used as controls, two of which previously analyzed by BeadChip.

A total of 2 µg of DNA was modified with bisulfite with EZ DNA Methylation kit (Zymo

Table 2. Primer sequences and PCR conditions used in the validation by pyrosequencing

Gene	Primer type	Primer sequence (5' to 3')	PCR conditions	Amplicon size (bp)
PRRT1	Forward	TTGGGTGGAGGAGGGATAA	95ºC (5'); 40 cycles [94ºC (30"), 64.4ºC (30"), 72ºC (30")]; 72ºC (10')	229
	Reverse	[Btn]ATAAACACCCCCCCAACTCTAACAA		
	Sequencing	GTGGGGGTTTTATTATTTTAG	NA	NA
RPS6KA4	Forward	GGGGAAATTGGTTTTAGGAGAG	95ºC (5'); 40 cycles [94ºC (30"), 62.5ºC (30"), 72ºC (30")]; 72ºC (10')	107
	Reverse	[Btn]CCCCATATCCAAAAAACTTAAAACCTTACT		
	Sequencing	ATTGGTTTTAGGAGAGG	NA	NA
WT1	Forward	TAGTAGGGGAGGTTGAGGG	95ºC (5'); 40 cycles [94ºC (30"), 65.6ºC (30"), 72ºC (30")]; 72ºC (10')	132
	Reverse	[Btn]ACTACTTCCCTTCCCCCTAAATAAAACTAT		
	Sequencing	GGGAGGTTGAGGGAG	NA	NA
AURKC	Forward	GTGGGTGTATGAGTTGTTTATTTTTATAA	95ºC (5'); 40 cycles [94ºC (30"), 63ºC (30"), 72ºC (30")]; 72ºC (10')	244
	Reverse	[Btn]AAAAAATACTTCCTAACTAACTCCTATTA		
	Sequencing	TTTGGTTTTAGTTTTTAGTG	NA	NA
TP73	Forward	TGTGTTTAAAATTGTTTTAGGAGGTAG	95ºC (5'); 40 cycles [94ºC (30"), 54.7ºC (30"), 72ºC (30")]; 72ºC (10')	108
	Reverse	[Btn]ATAACTAAACCTTTCCTAAAACCTATA		
	Sequencing	ATTGTTTTAGGAGGTAGG	NA	NA

Abbreviations: Btn: biotin; NA: not applicable

Research) according to the manufacturer's instructions and used in pyrosequencing reactions. Primers, complementary to the bisulfite-modified DNA sequences of *PRRT1* (Proline-Rich Transmembrane Protein 1), *RPS6KA4* (Ribosomal Protein S6 Kinase), *WT1*, *AURKC* (Aurora Kinase C) and *TP73* (Tumor Protein P73) were designed with PyroMark Q96 MDx v.1.0.6. (QIAGEN). Fragments spanning all regions were amplified with primers and conditions listed in Table 2. PCR mixtures contained 30 ng of modified DNA, 7.5. pmol of each primer (Sigma-Aldrich), 7.5. mM dNTPs, 5 µl of PCR buffer (Invitrogen) and 0.5. U of Taq DNA polymerase High Fidelity (Invitrogen) in final volumes of 50 µl. Single-stranded DNA templates and pyrosequencing were processed and run according to the manufacturer's protocol (QIAGEN) in a PyroMark Q96 platform (QIAGEN). PCR products were pyrosequenced with the specific sequencing primers listed in Table 2. CpG peaks were analyzed with PyroMark Q96 ID Software 2.5. (QIAGEN). The Methylation Index (MI) corresponded to the mean methylation level of all CpGs per gene. Two adjacent CpG sites to the one assessed by BeadChip were analyzed for *TP73,* and three were analyzed for *PRRT1*, *WT1* and *AURKC*. Due to difficulties in designing primers inside the *RPS6KA4* region tested with the BeadChip probe, the specific CpG interrogated by the probe was not validated although three adjacent sites were assessed.

3.5. Pyrosequencing data - statistical analyses

Statistical analyses were performed with GraphPad Prism 5 (GraphPad Software, USA); p values below 0.0.5 were considered to be statistically significant. Unpaired t-test or Mann-Whitney was used, according to the distribution of data. Receiver operating characteristic (ROC) curves were plotted for testing the potential use of gene methylation levels as distinctive markers.

4. RESULTS

4.1. Identification and validation of differentially methylated probes in WT

Initially, we evaluated whether DNA methylation profiles were capable of discriminating between tumors and normal kidney. Principal Component Analysis (PCA) showed that Principal Component 1 accounted for most of the variation (25.3.%), clearly discriminating WT from normal kidney (fig1A.jpg). This analysis also showed a highly heterogeneous methylation profile between WT samples, further indicated by Principal Component 2, accounting for 17.6.% of the remaining variation and separating the tumor sample from patient 20. This patient was diagnosed with unilateral WT at 137 months and presented approximately ten café au lait

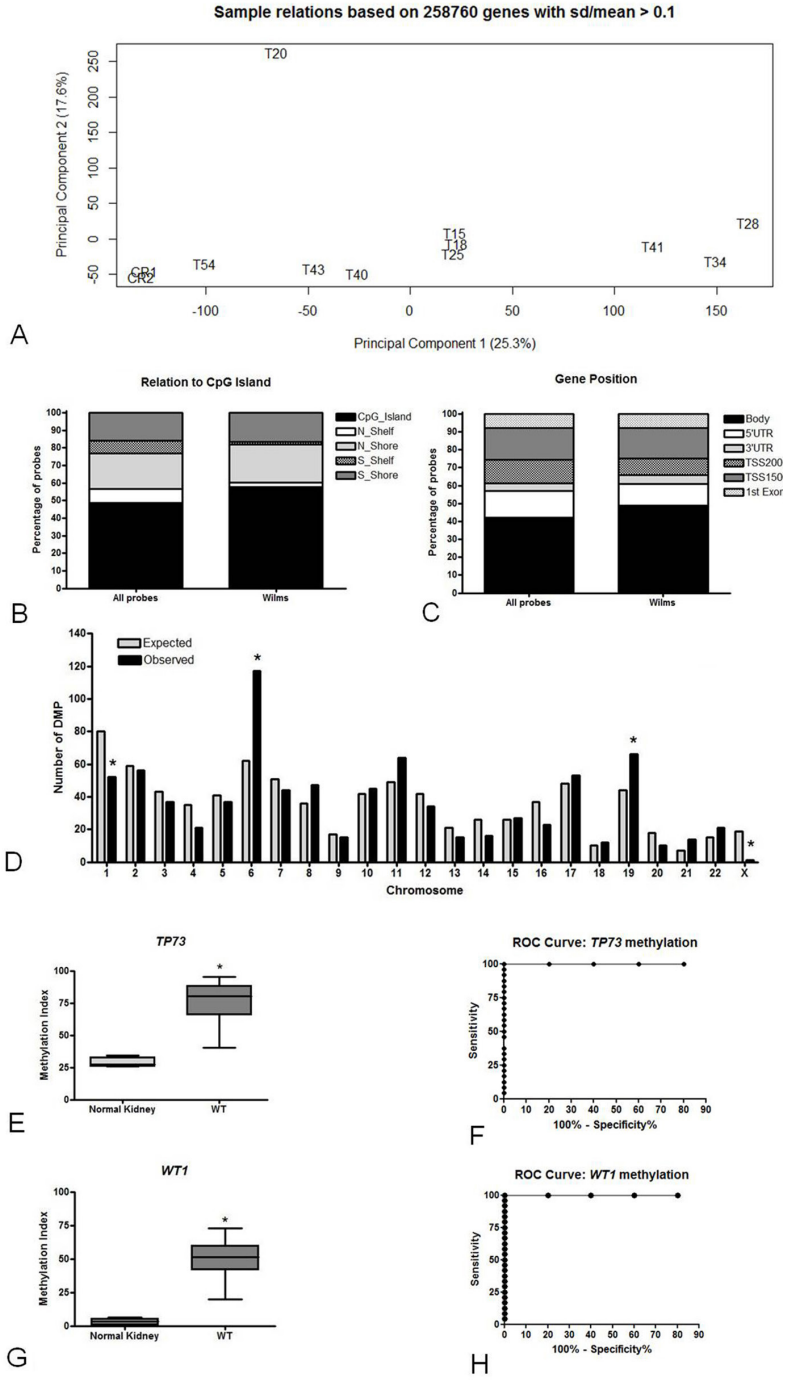

Figure 1. Global DNA methylation profile in Wilms Tumor. (A) Principal Component Analysis showing sample clustering according to the methylation levels of the 258,760 most variable probes between samples. Principal Component 1 accounted for 25.3.% of the observed variation, while Principal Component 2 accounted for 17.6.% of the remaining variation. CR = control (normal kidney samples); T = tumors. (B) Distribution of all probes included in the BeadChip array and probes found to be differentially methylated in WT with respect to normal kidney (adjusted p-value below 0.0.5) according to their distance to CpG islands. (C) Distribution of all probes included in the BeadChip array and probes found to be differentially methylated in WT with respect to normal kidney (adjusted p-value below 0.0.5) according to their position in genes. (D) Chromosome enrichment of DMPs between normal kidney and WT (adjusted p-value below 0.0.5). The graph represents the expected number of probes to be randomly altered in each chromosome (light gray bars) and the number of probes found to be differentially methylated between normal kidney and WT (black bars). Fisher's exact test, *p-value below 0.0.5. (E) Methylation profile of *TP73* 3'UTR evaluated by pyrosequencing in WT and normal kidney, *p-value below 0.0.5. (F) Receiver operating characteristic curve for discriminating between normal kidney and WT, according to methylation level of the *TP73* enhancer at the 3'UTR. For a *TP73* methylation index cut-off of 37.4.8%, the area under the curve was 1.0., with 100% sensitivity and specificity, p = 0.0.006. (G) Methylation profile of *WT1* enhancer evaluated by pyrosequencing in WT and normal kidney. *p-value below 0.0.5. (H) Receiver operating characteristic curve for the discrimination of normal kidney and WT, according to *WT1* enhancer methylation. For a *WT1* methylation index cut-off of 13.1.6%, the area under the curve was 1.0., with 100% sensitivity and specificity; p = 0.0.00567.

spots, although without any marked differences with respect to other patients.

Supervised analysis identified 827 differentially methylated probes in tumors respective to normal kidneys, comprising 277 hypomethylated (33.5.%) and 550 hypermethylated (66.5.%) CpG sites. These probes were subsequently classified according to their relation to CpG islands, as shown in fig1B.jpg. When comparing the distribution of differentially methylated probes (DMP) with the distribution of all probes analyzed by BeadChip, CpG islands were overrepresented (57.5. *vs* 48,5%) followed by underrepresentation of N_Shelves (2.8. *vs* 8.0.%) and S_Shelves (1.2. *vs* 7.2.%). In addition, island-specific probes were most frequently hypermethylated in WT (87%).

Subsequently, DMPs were classified according to gene regions. A comparison of their distribution respective with all probes showed overrepresentation in gene bodies (48.7. *vs* 42%) with underrepresentation in 5'UTRs (12.0. *vs* 15.0.%) and regions 200 bp apart from transcription start sites - TSS200 (9.0. *vs* 13.0.%) (fig1C.jpg). Finally, chromosome enrichment revealed a higher number of DMPs than randomly expected in chromosomes 6 and 19, while chromosome 1 and the X chromosome showed a significantly lower number of DMPs (fig1D.jpg).

All 10 tumor samples showed hypermethylation in the *TP73* 3'UTR, a profile validated by pyrosequencing in a larger and independent sample set (fig1E-F.jpg). A total of three CpG sites localized in the 3'UTR of *TP73* showed median methylation of 27.5.6% (25.5.9-34.5.5) in normal kidney against 80.2.3% (40.4.1-95.2.0) in WT ($p = 0.0.007$; fig1E.jpg). Moreover, *TP73* methylation discriminated WT from normal kidney with 100% sensitivity and specificity with a cut-off of 37.4.8% ($p = 0.0.006$; Figure 1F). Finally, WT samples from patients with bilateral tumors showed significant lower median methylation levels of *TP73* (65.6.%) than patients with unilateral WT (median = 85.8.%; $p = 0.0.25$, data not shown). For all other clinical-pathological characteristics, statistically significant associations were not observed.

Pyrosequencing analysis of the methylation profile of four CpG sites in a 50 Kb upstream enhancer of *WT1* confirmed hypermethylation in WT (median methylation = 51.3.%) respective to normal kidney (median methylation = 3.2.%; p below 0.0.001; fig1G.jpg) without any statistically significant associations with clinical-pathological characteristics. Finally, with a 13.1.6% cut-off, the methylation levels of these CpG sites discriminated WT from normal kidney with 100% sensitivity and specificity ($p = 0.0.00567$; fig1H.jpg).

4.2. Identification and validation of differentially methylated regions in WT

Thirty differentially methylated regions (DMRs) were identified in tumors with respect to normal kidney (Table 3). Mean DMR size was 432 bp, ranging from 157 to 4,480 bp, with a mean number of six DMPs per DMR (5-26). Similarly to previously observed in chromosome enrichment, chromosome 6 was one of the most frequently affected chromosomes.

Two novel DMRs were identified, one in chromosomes 11 and another in chromosome 19, in addition to the two DMRs (DMR1 and DMR2) previously reported in the literature (Table 3). The novel DMR identified by BeadChip in chromosome 11 (named DMR3), located within the gene body of *RPS6KA4* (Ribosomal protein S6 kinase A4), encompassing *MIR1237* (microRNA 1237), extending for 1,325 bp, was defined by 11 hypermethylated probes in WT (fig2A.jpg). Validation by pyrosequencing in the validation cohort (fig2C.jpg) confirmed that this region was hypermethylated in WT (median methylation = 81.9.8%) with respect to normal kidney (median methylation = 59.5.8%; $p = 0.0.092$). The novel DMR identified by BeadChip in chromosome 19 (named DMR4; fig2B.jpg) was defined by eight hypermethylated probes encompassing 227 bp within the *AURKC* promoter. These alterations were validated in the validation cohort (fig2D.jpg) in which the *AURKC* promoter was hypermethylated (median methylation = 92.1.1%) with respect to normal kidney (median methylation = 70.6.7%; $p = 0.0.007$). Interestingly, DMR4 status discriminated between WT and normal kidney with 100% sensitivity and specificity with a cut-off of 79.7.1% ($p = 0.0.006$; fig2E.jpg).

Within DMR1 (in 6p22.1.) and DMR2 (in 6p21.3.2), *ZNF311* and *PRRT1* were the most frequently altered genes, respectively. Validation of alterations in DMR2 by pyrosequencing confirmed the methylation profile of *PRRT1* previously identified with BeadChip, with higher methylation levels in tumors (median methylation = 81.8.9%) than in normal kidney (median methylation = 20.7.7%; fig2F.jpg).

5. DISCUSSION

Pediatric cancer has been extensively shown to differ from adult cancer in type and by its mainly unknown etiology, molecular mechanisms involved in development and progression, and relatively low number of somatic mutations (29). Most pediatric cancers probably result from disruption of cell differentiation, with epigenetic alterations, rather than mutations, playing a central role in inducing changes in cell morphology. Within this context, WT represents an interesting model for evaluating the role of epigenetic alterations in tumor development in childhood.

Table 3. Description of the differentially methylated regions in WT with respect to normal kidney

Chromosome	Start	End	Size (bp)	Number of altered probes	Minimum adjusted p-value	Methylation status in WT	EntrezID	Gene symbol	Distance to TSS	Promoter	DMR nomenclature
2	238707236	238707589	353	6	0.006	Hypermethylated	375316	*RBM44*	0	TRUE	
2	208635605	208636032	427	6	0.021	Hypermethylated	7855	*FZD5*	-1462	TRUE	
2	20441905	20442210	305	5	0.025	Hypermethylated	23369	*PUM2*	36370	FALSE	
3	156838096	156838403	307	5	0.019	Hypermethylated	339894	*LINC00880*	2388	FALSE	
5	180622072	180622643	571	5	0.016	Hypermethylated	81786	*TRIM7*	5287	FALSE	
6	144508118	144508735	617	5	0.006	Hypermethylated	8676	*STX11*	36464	FALSE	
6	27173574	27173991	417	5	0.021	Hypermethylated	10279	*PRSS16*	-41511	FALSE	
6	28956226	28956989	763	22	0.029	Hypermethylated	282890	*ZNF311*	15002	FALSE	DMR1*
6	32116538	32117565	1027	26	0.035	Hypermethylated	80863	*PRRT1*	2135	FALSE	DMR2*
6	32908567	32909003	436	8	0.042	Hypomethylated	3109	*HLA-DMB*	0	TRUE	
6	32115964	32116225	261	9	0.043	Hypermethylated	80863	*PRRT1*	3475	FALSE	
6	35109242	35109548	306	8	0.044	Hypermethylated	6954	*TCP11*	-55	TRUE	
6	168197505	168198163	658	8	0.049	Hypermethylated	26238	*LINC01558*	0	TRUE	
8	22132563	22133076	513	12	0.006	Hypermethylated	55124	*PIWIL2*	0	TRUE	
8	41167660	41168264	604	10	0.025	Hypermethylated	6422	*SFRP1*	-670	TRUE	
8	105379368	105379726	358	5	0.046	Hypermethylated	81501	*DCSTAMP*	27344	FALSE	
10	22622459	22623460	1001	5	0.014	Hypermethylated	648	*BMI1*	12320	FALSE	
10	88296171	88296809	638	5	0.026	Hypermethylated	23063	*WAPAL*	-14630	FALSE	
11	64135650	64136975	1325	11	0.003	Hypermethylated	100302280	*RPS6KA4/ MIR1237*	0	TRUE	DMR3
11	64863151	64863611	460	5	0.024	Hypermethylated	738	*VPS51*	0	TRUE	
11	69982916	69987414	4498	5	0.043	Hypomethylated	55107	*ANO1*	28457	FALSE	
12	51236582	51236768	186	6	0.012	Hypermethylated	283471	*TMPRSS12*	0	TRUE	
12	107974296	107974733	437	8	0.031	Hypermethylated	121551	*BTBD11*	0	TRUE	
12	12509705	12509963	258	6	0.050	Hypomethylated	503693	*LOH12CR2*	38	FALSE	
16	83986702	83986941	239	5	0.046	Hypomethylated	29948	*OSGIN1*	0	TRUE	
17	36997420	36997740	320	7	0.011	Hypermethylated	388381	*C17orf98*	0	TRUE	
19	57742217	57742444	227	8	0.035	Hypermethylated	6795	*AURKC*	0	TRUE	DMR4
21	35831871	35832028	157	6	0.031	Hypomethylated	3753	*KCNE1*	0	TRUE	
22	19750918	19751899	981	5	0.018	Hypermethylated	6899	*TBX1*	6692	FALSE	
22	25159879	25160308	429	5	0.042	Hypermethylated	440822	*PIWIL3*	10379	FALSE	

Abbreviations: TSS: transcription start site; DMR: differentially methylated region, *DMRs previously shown to be hypermethylated in WT (11).

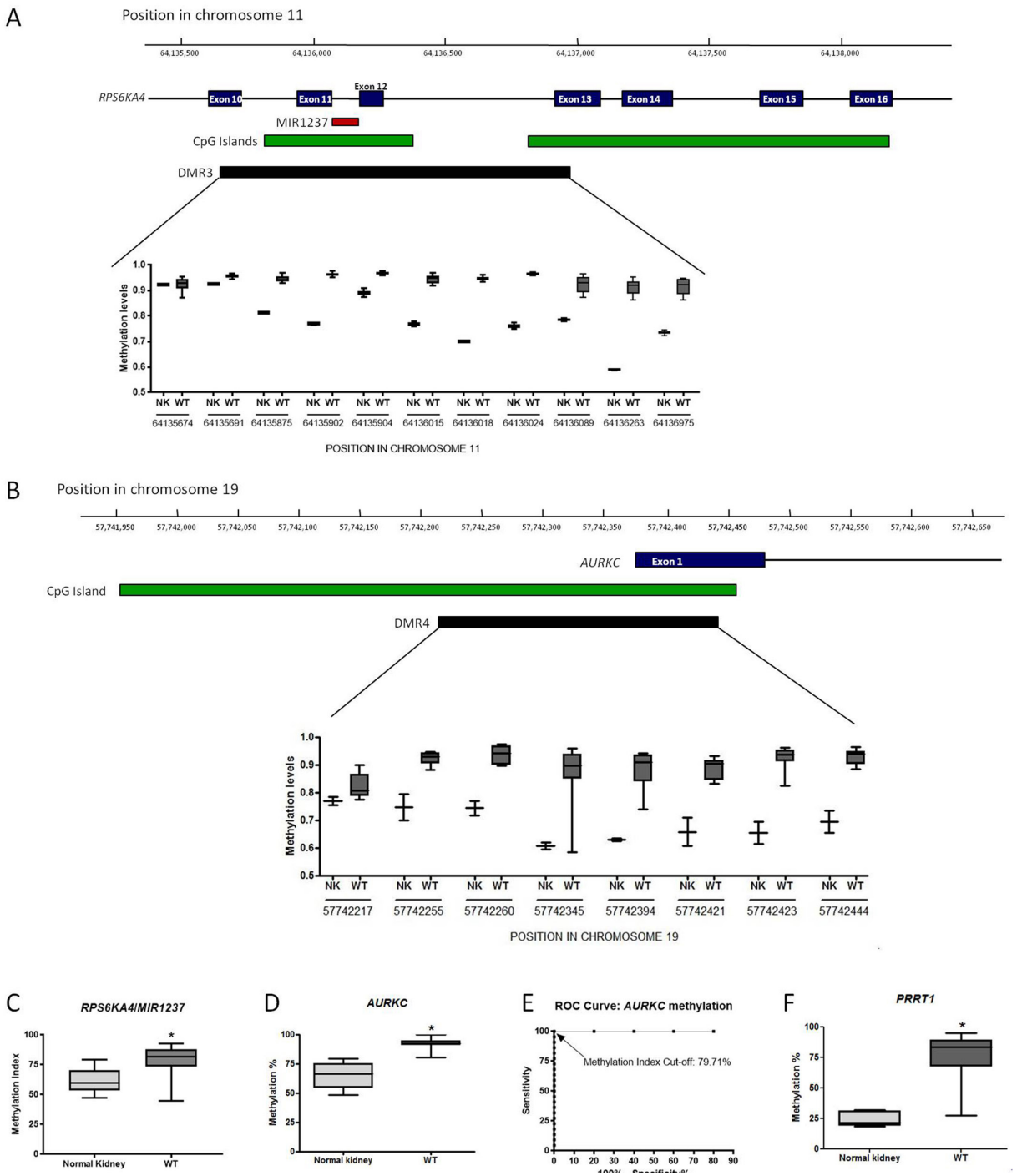

Figure 2. Differentially methylated regions in Wilms Tumor. (A) Schematic representation of DMR3 in *RPS6KA4*/*MIR1237*, found to be hypermethylated in WT with respect to normal kidney (NK). This DMR is located within two CpG islands (green bars) partially overlapping the *RPS6KA4* gene body and encompassing *MIR1237* (red bar), comprising 11 BeadChip probes. The methylation profile of these probes in WT and NK is represented in the box-plot located at the bottom. Each probe assesses the methylation level each CpG site in chromosome 11 depicted under the box-plot. Representation adapted from Genome Browser (http://genome.ucsc.edu/), according to GRCh37/hg19. (B) Schematic representation of the DMR in the *AURKC* promoter region found to be hypermethylated in WT with respect to normal kidney (NK). This DMR is located in the CpG island (green bar) overlapping *AURKC* exon 1 (blue bar), encompassing eight probes tested by the BeadChip array. The methylation profile of these probes in WT and NK is represented in the box-plot located at the bottom of the figure. Each probe assesses the methylation levels of one CpG site, whose position in chromosome 19 is depicted under the box-plot. Representation adapted from Genome Browser (http://genome.ucsc.edu/), according to GRCh37/hg19. (C) Methylation profile of the *RPS6KA4*/*MIR1237* DMR (DMR3) confirmed by pyrosequencing in WT and normal kidney. (D) Methylation profile of *AURKC* DMR (DMR4) confirmed by pyrosequencing in WT and normal kidney. (E) Receiver operating characteristic curve for the discrimination of normal kidney and WT, according to *AURKC* DMR methylation. For a *AURKC* methylation index cut-off of 79.7.1%, the area under the curve was 1.0., with 100% sensitivity and specificity, p = 0.0.006. (F) Methylation profile of *PRRT1* DMR confirmed by pyrosequencing in WT and normal kidney. *p-value below 0.0.5.

Somatic mutations have been found in less than 50% of WT, while approximately 70% display loss of 11p15 imprinting resulting in biallelic *IGF2* expression. The relevance of these findings has been underlined by the experimental induction of murine nephroblastoma following *IGF2* overexpression (30), although several authors have reported that epigenetic alterations are not limited to the *IGF2*/*H19* locus (10,11,31).

In this study, comparisons of the overall DNA methylation profile of WT and normal kidney showed hypermethylation in 66.5.% of 827 DMPs, mainly in CpG islands, while a high frequency of DMPs was identified in genes bodies. Epigenetic alterations of these regions have been for a long time disregarded, although recent reports indicated that they may affect expression by controlling transcription elongation, regulatory regions like enhancers as well as splicing (32). The hypermethylation profile observed in our study, more frequently affecting CpG islands, was consistent with the silencing of tumor suppressor genes reported in different tumors. On the other hand, the global hypomethylation profile characteristic of solid tumors largely affects non-genic regions, mainly those associated with mobile elements and not assessed by BeadChip.

One specific probe was identified in an enhancer located in the 3'UTR of *TP73* which was hypermethylated in all WT samples. The effects of epigenetic alterations in enhancers or 3'UTRs are poorly understood. Enhancer methylation has been associated to regulation of trans-activating factors binding which regulate transcriptional elongation (33), while 3'UTR methylation might have similar effects to the methylation of promoters (34). It is therefore likely that the hypermethylated region of *TP73* must have resulted in downregulating the expression of this gene, in agreement with a report showing lower *WWOX* expression in WT consequently to promoter methylation positively correlated with *TP73* expression (35). On the other hand, hypomethylation of the *TP73* promoter and its higher expression have also been reported in WT. These findings, however, suggested that *TP73* is likely to play a role in WT development, although the regulatory mechanisms involved in this process are still poorly understood.

In this study, hypermethylation was detected in an enhancer region located approximately 50 kb upstream of *WT1* in all 24 analyzed WT samples, providing evidence that this epigenetic alteration might be playing a role in *WT1* inactivation and gene expression. Interestingly, a recent study on gene expression in differentiation of murine Sertoli cells showed a peak of DNaseI hypersensitive sites 50 kb upstream of *Wt1,* in a similar region herein identified. Furthermore, this region was unique to Sertoli cells and associated to H3K27ac, suggesting that it functioned as an active enhancer for *Wt1* in these cells (36).

In this study, comparisons between WT and normal kidney showed thirty DMRs. Two of these (DMR1 and DMR2) have been previously reported and found to correctly discriminate between normal kidney and WT as well as between aggressive and intermediate risk tumors in 98% of WT, while DMR2 hypermethylation was validated as a biomarker of response to treatment in cell-free circulating DNA (11). The third DMR identified by Charlton *et al*. (11) was not detected in this study, probably a consequence of the low number of samples and/or the different methods and parameters herein used for identifying DMRs. One novel DMR herein identified (DMR3, within the *RPS6KA4* gene body and encompassing *MIR1237*), was hypermethylated in WT. *RPS6KA4,* a member of the ribosomal S6 kinase family, encodes a serine/threonine kinase shown to phosphorylate different target proteins, including H3K27me3 (tri-methylated lysine 27 on histone H3), leading to displacement of polycomb proteins and subsequent gene activation (37). However, no evidence of *RPS6KA4* regulation by DNA methylation has been so far reported contrary to *MIR1237* expression that has recently been shown to be regulated by the methylation status of its 5' CpG island in gastric cancer (38). In this report, proto-oncogenes were identified as MIR1237 targets, including the receptor tyrosine kinase *ERBB3* (erb-b2 receptor tyrosine kinase 3) and *CCND2* (cyclin D2), suggesting that this microRNA was a tumor suppressor. DMR4 (in the *AURKC* promoter) was also hypermethylated in WT with respect to normal kidney. To date, a study analyzing methylation at the *AURKC* promoter and gene expression showed an inverse correlation between them in cancer cell lines and tumors, including renal clear cell carcinoma, while lower *AURKC* expression was associated with advanced stages of colon adenocarcinoma (39). *AURKC* is a member of the Aurora kinase family that includes two other members *AURKA* and *AURKB*. While AURKA and B are widespread throughout the body, AURKC seems to be restricted to meiotic cells and plays a role in fertility, and its dysregulation in cancer may be related to alterations of centrosome and telomere length (40).

In this study, we reinforced the relevance of alterations of DNA methylation in Wilms Tumor. Some changes were detected in all patients and, although restricted to a limited sample, they were indicative that they were intimately related to this malignancy. We cannot rule out the influence of chemotherapy on our molecular findings because it is not a common practice to take biopsies prior to treatment. Analyses of the methylation profile of DMRs in nephrogenic rests, considered as WT precursor lesions, showed intermediate methylation levels between normal kidney

and tumors, leading to the proposition that these alterations could be associated with transformation of embryonic cells to a malignant phenotype (11). Although we cannot extrapolate this finding, the fact that two previously reported DMRs were also found in our study suggested that these alterations might be involved in tumor development rather than a consequence of exposure to chemotherapy.

On the other hand, a high heterogeneity was observed among tumors, as shown by PCA, pointing to the complex nature of aberrant DNA methylation patterns in cancer, affecting not only promoter regions, but enhancers, UTRs and gene bodies. These findings might shed light to novel regulatory mechanisms and players in tumor development, as was the case of *AURKC, RPS6KA4,* and *MIR1237* in WT.

6. ACKNOWLEDGEMENTS

Hanna S Pereira and Sheila C Soares Lima contributed equally to this work. Work supported by INCT para Controle do Câncer (CNPq grant 573806/2008-0 and FAPERJ grant E26/170.0.26/2008).

7. REFERENCES

1. R. Scott, C. Stiller, L. Walker, N. Rahman: Syndromes and constitutional chromosomal abnormalities associated with Wilms tumour. *J Med Genet* 43(9), 705–715 (2006) DOI: 10.1136/jmg.2006.041723

2. M. Rivera, W. Kim, J. Wells, D. Driscoll, B. Brannigan, M. Han, J. Kim, A. Feinberg, W. Gerald, S. Vargas, L. Chin, A. Iafrate, D. Bell, D. Haber: An X chromosome gene, WTX, is commonly inactivated in Wilms tumor. *Science* 315(5812), 642–645 (2007) DOI: 10.1126/science.1137509

3. M. Maschietto, B. de Camargo, H. Brentani, P. Grundy, S. Sredni, C. Torres, L. Mota, I. Cunha, D. Patrão, C. Costa, F. Soares, R. Brentani, D. Carraro: Molecular profiling of isolated histological components of Wilms' tumor implicates a common role for the Wnt signaling pathway in kidney and tumor development. *Oncology* 75(1-2), 81–91 (2008) DOI: 10.1159/000155210

4. J. Beckwith, N. Kiviat, J. Bonadio: Nephrogenic rests, nephroblastomatosis, and the pathogenesis of Wilms' tumor. *Fetal Pediatr Pathol* 10(1-2), 1–36 (1990) DOI: 10.3109/15513819009067094

5. J. Dome, E. Perlman, N. Graf: Risk stratification for Wilms tumor: current approach and future directions. *Am Soc Clin Oncol Educ Book*, 215–223 (2014). DOI: 10.14694/EdBook_AM.2014.34.215

6. R. Scott, A. Murray, L. Baskcomb, C. Turnbull1, C. Loveday, R. Al-Saadi, R. Williams, F. Breatnach, M. Gerrard, J. Hale, J. Kohler, P. Lapunzina, G. Levitt, S. Picton, B. Pizer, M. Ronghe, H. Traunecker, D. Williams, A. Kelsey, G. Vujanic, N. Sebire, P. Grundy, C. Stiller, K. Pritchard-Jones, J. Douglas, N. Rahman: Stratification of Wilms' tumor by genetic and epigenetic analysis. *Oncotarget* 3(3), 327-335 (2012) DOI: 10.18632/oncotarget.468

7. E. Ruteshouser, S. Robinson, V. Huff: Wilms' tumor genetics: mutations in WT1, WTX, and CTNNB1 account for only about one-third of tumors. *Genes Chromosomes Cancer* 47(6), 461–470 (2008) DOI: 10.1002/gcc.20553

8. G. Torrezan, E. Ferreira, A. Nakahata, B. Barros, M. Castro, B. Correa, A. Krepischi, E. Olivieri, I. Cunha, U. Tabori, P. Grundy, C. Costa, B. de Camargo, P. Galante, D. Carraro: Wilms Recurrent somatic mutation in DROSHA induces microRNA profile changes in Wilms tumour. *Nat Commun* 5, 4039 (2014) DOI: 10.1038/ncomms5039

9. N. Bardeesy, D. Falkoff, M. Petruzzi, N. Nowak, B. Zabel, M. Adam, M. Aguiar, P. Grundy, T. Shows, J. Pelletier: Anaplastic Wilms' tumour, a subtype displaying poor prognosis, harbours p53 gene mutations. *Nat Genet* 7(1), 91-97 (1994) DOI: 10.1038/ng0594-91

10. J. Charlton, R. Williams, N. Sebire, S. Popov, G. Vujanic, T. Chagtai, M. Alcaide-German, T. Morris, L. Butcher, P. Guilhamon, S. Beck, K. Pritchard-Jones: Comparative methylome analysis identifies new tumour subtypes and biomarkers for transformation of nephrogenic rests into Wilms tumour. *Genome Med* 7(1), 11 (2015) DOI: 10.1186/s13073-015-0136-4

11. J. Charlton, R. Williams, M. Weeks, N. Sebire, S. Popov, G. Vujanic, W. Mifsud, M. Alcaide-German, L. Butcher, S. Beck, K. Pritchard-Jones: Methylome analysis identifies a Wilms' tumor epigenetic

biomarker detectable in blood. *Genome Biol* 15(8), 434 (2014)
DOI: 10.1186/s13059-014-0434-y

12. R. Scott, J. Douglas, L. Baskcomb, A. Nygren, J. Birch, T. Cole, V. Cormier-Daire, D. Eastwood, S. Garcia-Minaur, P. Lupunzina, K. Tatton-Brown, J. Bliek, E. Maher, N. Rahman: Constitutional 11p15 abnormalities, including heritable imprinting center mutations, cause nonsyndromic Wilms tumor. *Nat Genet* 40(11), 1329–1334 (2008)
DOI: 10.1038/ng.243

13. L. Cardoso, J. Castaño, H. Pereira, M. Lima, A. Santos, P. Faria, S. Ferman, H. Abreu, J. Nevado, J. Almeida, P. Lapunzina, F. Vargas: Constitutional and somatic methylation status of DMRH19 and KvDMR in Wilms' tumor patients. *Genet Mol Biol* 35(4), 714–724 (2012)
DOI: 10.1590/S1415-47572012005000073

14. K. Wagner, W. Cooper, R. Grundy, G. Caldwell, C. Jones, R. Wadey, D. Morton, P. Schofield, W. Reik, F. Latif1, E. Maher: Frequent RASSF1A tumour suppressor gene promoter methylation in Wilms' tumour and colorectal cancer. *Oncogene* 21(47), 7277-7282 (2002)
DOI: 10.1038/sj.onc.1205922

15. J. Hubertus, F. Zitzmann, F. Trippel, J. Muller-Ho, M. Stehr, D. von Schweinitz, R. Kappler: Selective methylation of CpGs at regulatory binding sites controls NNAT expression in Wilms tumors. *PLoS One* 8(6), e67605 (2013)
DOI: 10.1371/journal.pone.0067605

16. K. Malik, A. Salpekar, A. Hancock, K. Moorwood, S. Jackson, A. Charles, K. Brown: Identification of differential methylation of the WT1 antisense regulatory region and relaxation of imprinting in Wilms' tumor. *Cancer Res* 60(9), 2356–2360 (2000)

17. M. Ehrlich, N. Hopkins, G. Jiang, J. Dome, M. Yu, C. Woods, G. Tomlinson, M. Chintagumpala, M. Champagne, L. Dillerg, D. Parham, J. Sawyer: Satellite DNA hypomethylation in karyotyped Wilms tumors. *Cancer Genet Cytogenet* 141(2), 97–105 (2003)
DOI: 10.1016/S0165-4608(02)00668-4

18. A. Feinberg, R. Ohlsson, S. Henikoff: The epigenetic progenitor origin of human cancer. *Nat Rev Genet* 7(1), 21–33 (2006)
DOI: 10.1038/nrg1748

19. S. Bhatnagar: Management of Wilms' tumor: NWTS vs SIOP. *J Indian Assoc Pediatr Surg* 14(1), 6–14 (2009)
DOI: 10.4103/0971-9261.54811

20. J. Sambrook, M. Green. Isolation and Quantification of DNA. In: Molecular Cloning: A laboratory manual, third ed. vol 1. Eds: Cold Spring Harbor Laboratory Press, New York (2001)
DOI: 10.3724/SP.J.1141.2012.01075

21. Team, Rs. RStudio: Integrated Development for R (2015) at http://www.rstudio.com/

22. S. Davis, P. Du, S. Bilke, J. T. Triche, M. Bootwalla: Methylumi: Handle Illumina methylation data. R package (2015)

23. Y. Chen, M. Lemire, S. Choufani, D. Butcher, D. Grafodatskaya, B. Zanke, S. Gallinger, T. Hudson, R. Weksberg: Discovery of cross-reactive probes and polymorphic CpGs in the Illumina Infinium HumanMethylation450 microarray. *Epigenetics* 8(2), 203–209 (2013)
DOI: 10.4161/epi.23470

24. R. Pidsley, C. Wong, M. Volta, K. Lunnon, J. Mill, L. Schalkwyk: A data-driven approach to preprocessing Illumina 450 K methylation array data. *BMC Genomics* 14, 293 (2013)
DOI: 10.1186/1471-2164-14-293

25. P. Du, W. Kibbe, S. Lin: lumi: A pipeline for processing Illumina microarray. *Bioinformatics* 24(13), 1547–1548 (2008)
DOI: 10.1093/bioinformatics/btn224

26. M. Aryee1, A. Jaffe, H. Corrada-Bravo, C. Ladd-Acosta, A. Feinberg, K. Hansen, R. Irizarry: Minfi: A flexible and comprehensive Bioconductor package for the analysis of Infinium DNA methylation microarrays. *Bioinformatics* 30(10), 1363–1369 (2014)
DOI: 10.1093/bioinformatics/btu049

27. M. Ritchie, B. Phipson, D. Wu, Y. Hu, C. Law, W. Shi, G. Smyth: Limma powers differential expression analyses for RNA-sequencing and microarray studies. *Nucleic Acids Res* 43(7), e47 (2015)
DOI: 10.1093/nar/gkv007

28. P. Du, R. Bourgon: MethyAnalysis: an R package for DNA methylation data analysis and visualization. R package version 1.1.8.0. (2017)

29. B. Vogelstein, N. Papadopoulos, V. Velculescu, S. Zhou, L. Diaz, K. Kinzler:

Cancer genome landscapes. *Science* 339(6127), 1546–1558 (2013)
DOI: 10.1126/science.1235122

30. Q. Hu, F. Gao, W. Tian, E. Ruteshouser, Y. Wang, A. Lazar, J. Stewart, L. Strong, R. Behringer, V. Huff1: Wt1 ablation and Igf2 upregulation in mice result in Wilms tumors with elevated ERK1/2 phosphorylation. *J Clin Invest* 121(1), 174–183 (2011)
DOI: 10.1172/JCI43772

31. D. Song, L. Yue, G. Wu, S. Ma, H. Yang, Q. Liu, D. Zhang, Z. Xia, J. Jia, J. Wang: Evaluation of promoter hypomethylation and expression of p73 as a diagnostic and prognostic biomarker in Wilms' tumour. *J Clin Pathol* 69(1), 12–18 (2015)
DOI: 10.1136/jclinpath-2015-203150

32. S. Lee, W. Choi, J. Lee, Y. Kim: The regulatory mechanisms of intragenic DNA methylation. *Epigenomics* 7(4), 527–531 (2015)
DOI: 10.2217/epi.15.38

33. A. Kazanets, T. Shorstova, K. Hilmi, M. Marques, M. Witcher: Epigenetic silencing of tumor suppressor genes: Paradigms, puzzles, and potential. *Biochim Biophys Acta* 1865(2), 275-288 (2016)
DOI: 10.1016/j.bbcan.2016.04.001

34. G. Maussion, J. Yang, M. Suderman, A. Diallo, C. Nagy, M. Arnovitz, N. Mechawar, G. Turecki: Functional DNA methylation in a transcript specific 3'UTR region of TrkB associates with suicide. *Epigenetics* 9(8), 1061-1070 (2014)
DOI: 10.4161/epi.29068

35. E. Płuciennik, M. Nowakowska, W. Wujcicka1, A. Sitkiewicz, B. kazanowska, E. Zielińska, A. Bednarek: Genetic alterations of WWOX in Wilms' tumor are involved in its carcinogenesis. *Oncol Rep* 28(4), 1417–1422 (2012)
DOI: 10.3892/or.2012.1940

36. D. Maatouk, A. Natarajan, Y. Shibata, L. Song, G. Crawford, U. Ohler, B. Capel: Genome-wide identification of regulatory elements in Sertoli cells. *Development* 144(4), 720-730 (2017)
DOI: 10.1242/dev.142554

37. S. Gehani, S. Agrawal-Singh, N. Dietrich, N. Christophersen, K. Helin, K. Hansen: Polycomb group protein displacement and gene activation through MSK-dependent H3K27me3S28 phosphorylation. Mol Cell 39(6), 886-900 (2010)
DOI: 10.1016/j.molcel.20http://dx.doi.org/10.08.020

38. J. Bae, M. Kang, K. Yang, T. Kim, J. Yi: Epigenetically silenced microRNAs in gastric cancer: Functional analysis and identification of their target genes. *Oncol Rep* 34(2), 1017-1026 (2015)
DOI: 10.3892/or.2015.4036

39. S. Fujii, V. Srivastava, A. Hegde, Y. Kondo, L. Shen, K. Hoshino, Y. Gonzalez, J. Wang, K. Sasai, X. Ma, H. Katayama, M. Estecio, S. Hamilton, I. Wistuba, J. Issa, S. Sem: Regulation of AURKC expression by CpG island methylation in human cancer cells. *Tumour Biol* 36(10), 8147–8158 (2015)
DOI: 10.1007/s13277-015-3553-5

40. S. Quartuccio, K. Schindler: Functions of Aurora kinase C in meiosis and cancer. *Front Cell Dev Biol* 3, 50 (2015)
DOI: 10.3389/fcell.2015.00050

Key Words: Wilms' tumor, DNA methylation, Differentially methylated regions, Aurora Kinase C, Enhancers

Send correspondence to: Hector N. Seuanez, Instituto Nacional de Cancer, Rua Andre Cavalcanti, 37, 20231-050 Rio Janeiro, RJ, Brazil, Tel: 55-21 3207 6582, Fax: 55 21 3207 6553, E-mail: hseuanez@inca.gov.br